



*Supplement of*

## **The influence of small farm reservoir network characteristics on their cumulative hydrological impacts**

**Henri Lechevallier et al.**

*Correspondence to:* Henri Lechevallier ([henri.lechevallier@inrae.fr](mailto:henri.lechevallier@inrae.fr))

The copyright of individual parts of the supplement might differ from the article licence.

## S 1 Relationship volume - area of reservoirs

To compute the evaporation on reservoirs, the model needs the current surface of reservoirs. The general shape of reservoirs is taken from the study of Liebe et al. (2005), and it corresponds to a reversed half-pyramid. With this geometry, volume ( $V'$ ) and area ( $A'$ ) are linked at any time step with the following relation:

$$A' = \left( \frac{V'}{V_{max}} \right)^{\frac{2}{3}} A_{max} \quad (1)$$

$V_{max}$  is the maximum volume ( $m^3$ ), and  $A_{max}$  is the maximum area ( $m^2$ ). Both are linked with a third parameter, the maximum depth of the reservoir ( $h_{max}$ , in  $m$ ):

$$V_{max} = \frac{1}{3} A_{max} h_{max} \quad (2)$$

In the numerical experiment, we decided to set the value of  $h_{max}$  to 4 m. This guaranties that, at fixed total capacity stored on the basin, the maximum area of reservoirs is the same.

## S 2 Complement to the representation of withdrawals and irrigation in the model

Each small reservoir is connected to a defined set of SU (surface units, i.e. fields), which will be irrigated if needed with water coming from the reservoir. Each day, irrigation needs on the connected SUs are determined based on a decision model (Murgue et al., 2014). The total water demand is compared to the available stock in the reservoir. If the stock is sufficient, all needs are covered. Otherwise, all available stock is used and distributed on the corresponding SU proportionally to demands and surfaces. The maximum stock for irrigation corresponds to 3/4 of reservoir total capacity. During a cropping season, total withdrawals can exceed this maximum stock if there is enough water flowing in the river to fill the reservoir during the season.

In the decision model, each crop is associated to a set of decision rules for irrigation in the form of a list of conditions to verify to trigger irrigation. The conditions are presented below and an example is provided in Table S1 for maize, soybean, and straw cereals:

- Current date is within the correct time window.
- Crop development stage is within the correct physiological window.
- Rainfall in the X previous day is less than the defined threshold.
- The field has not been irrigated for X days.
- Soil humidity is lower/higher than a defined threshold.

Table S1: Decision rules for irrigation for the main irrigated crops on the Gélon catchment. The rules have been simplified to fit in one summary table (there can be sub-periods with different parameters for each crop, and there are more than one rainfall threshold). Vscale is the vegetation scale and is an indicator of phylosiological crop development used in the model. A value of 1 corresponds to flowering.

Crop	Irrigation dose (mm)	Period of irrigation	Vscale range	Number of days between two irrigations	Rainfall threshold	Soil humidity threshold
Maize	30	20 mai - 20 september	0.9 - 2.5	7	25 mm in the last 3 days	0.5
Straw cereal	30	15 mai - 14 june	0.8 - 1.3	7	15 mm in the last 7 days	0.75
Soybeans	30	1 june - 15 september	0.45 - 1.4	7	30 mm in the last 3 days	0.75

Table 2 of the article presents the irrigable crops used in the numerical experiment, along with the irrigation period. Note that the irrigation period of sorghum is the same than that of straw cereals. In the model, sorghum was first considered as a straw cereal, which is not realistic. This will be changed in future uses of the model. For the numerical experiment, given the low proportion of sorghum, we can assume that this change will not affect the results.

## S 3 Complement to the method for reservoir distribution on the hydrological network

### S 3.1 The two pools of RS

Figure S1 shows the breakdown of the hydrological network into two pools of reach sections (RS). The used criteria is the maximum area drained by a first-order stream in the Strahler classification (Strahler, 1957). As a result, we can see that all first order streams are included in the upstream pool. After few confluences, the RS are associated to the downstream pool. This leads to two pools with different number of RS, but that are equilibrated in terms of network length. The main advantage is that they are defined with a morphological criteria, which results in a “natural” decomposition of the network.

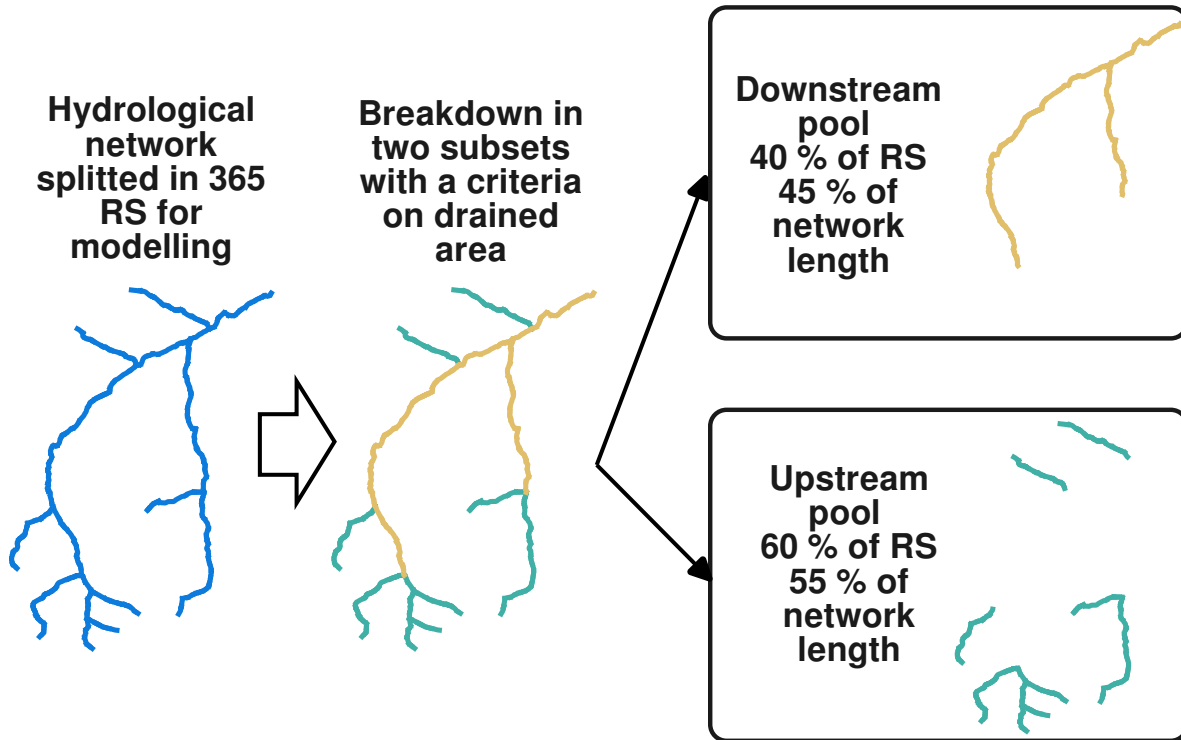


Figure S1: Method for the construction of the two subsets of reach sections (RS) and visualization of the two pools.

### S 3.2 Example of reservoir distributions on the hydrological network

Figure S2 shows three example of networks generated with our method. For the upstream network (S2a), most reservoirs are located on first order streams. For the downstream network (S2c), most reservoirs are located on the main channel. For the balanced network, there are reservoirs on first and higher order stream without clear majority.

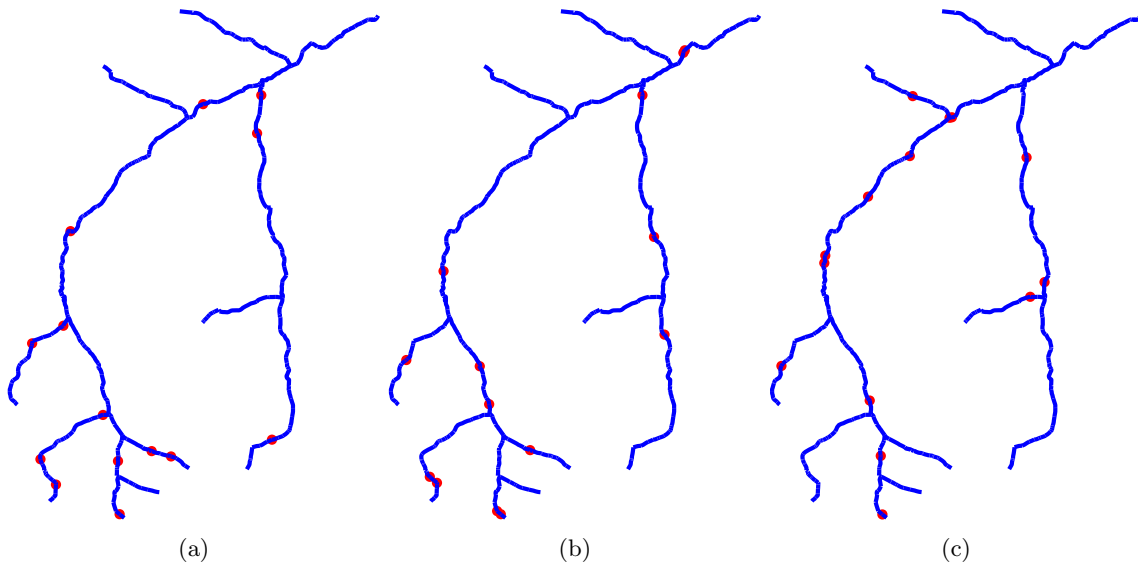


Figure S2: Example of three networks of reservoirs generated with the ustream (a), balanced (b), and downstream (c) method for the distribution along the stream.

### S 3.3 Characterization of produced networks of reservoirs in terms of drained area

We verified that our method for the random placement of the reservoirs led to contrasted situations in terms of the mean drained area of the reservoirs (Figure S3). There is only little overlapping between the boxes so we can consider that the method produces contrasted situations.

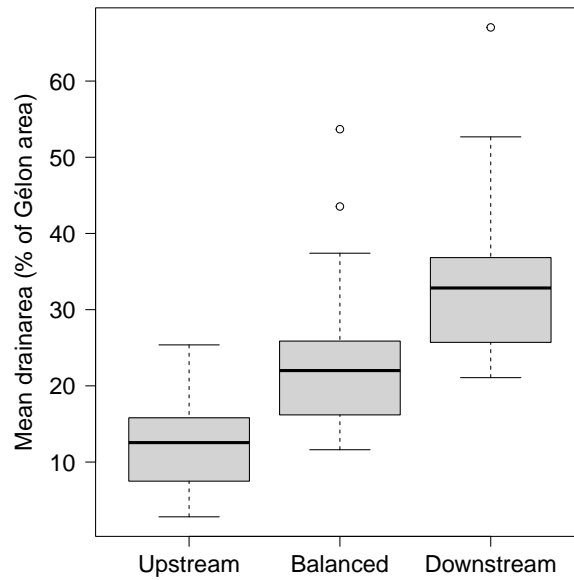


Figure S3: Boxplot of the mean drained area of the reservoirs in each situation depending on the method used for the placement of reservoir (n=30 per box).

## S 4 Complementary figures to the result section

### S 4.1 Comparison of seasonal withdrawals and evaporation in reservoirs

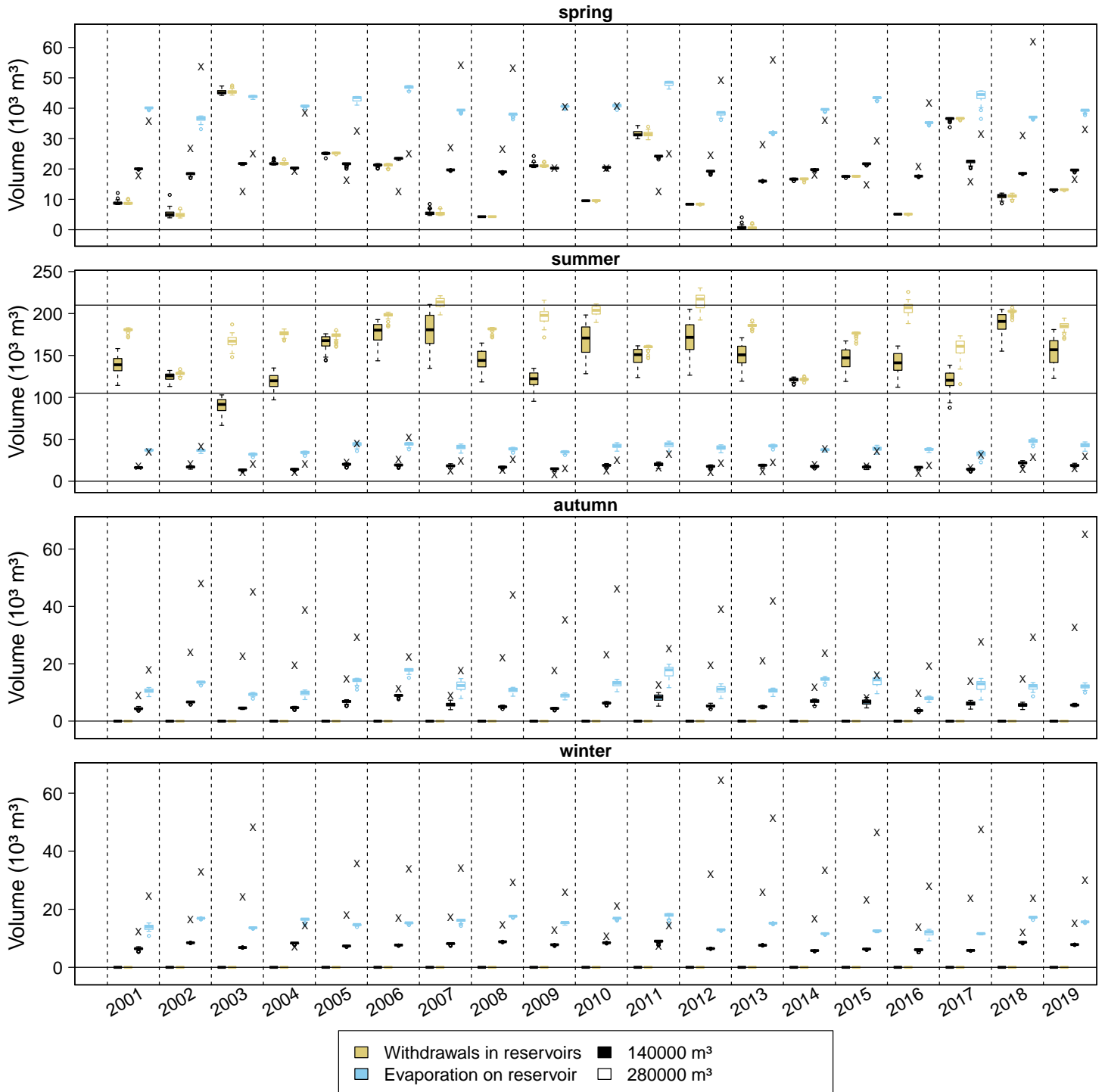


Figure S4: Boxplot of the seasonal withdrawals and evaporation on reservoirs for each value of total storage capacity.  $n=45$  per box. The black horizontal lines (in summer) indicate 3/4 of reservoir sizes. The x on the same columns as evaporation indicate the volume of rainfall on the reservoirs for the season.

Regarding the withdrawals in reservoirs, Figure S4 shows:

- The seasonality of withdrawals in reservoirs: there is no withdrawals in autumn and in winter, and withdrawals are much higher in summer than in spring.
- A low variability of withdrawals in spring between the different simulations. At the beginning of spring, reservoirs are usually full. The withdrawals in spring are lower than 3/4 of capacity threshold which means that they are not limited by the capacity of the reservoirs. Therefore, there is no reason that the withdrawals in spring vary between situations.
- A large variability of withdrawals in summer between the different simulations. The capacity is an important factor for the summer withdrawals as the range of variation of withdrawals are totally different for the two capacities. The variability is larger for the situations with 140000 m<sup>3</sup> of storage capacity than for situations with 280000 m<sup>3</sup> of storage capacity, which indicates that other factors also play for situations with lower capacities. The summer withdrawals exceed the 3/4 of capacity threshold for almost all years in situation with 140000 m<sup>3</sup> of storage capacity. It happens rarely for situations with 280000 m<sup>3</sup> of storage capacity.

The evaporation and rainfall on reservoirs are directly proportional to the total surface of reservoirs, and hence the total storage capacity. Between simulations with the same capacity, the variability of evaporation is generally low, lower than the variability of withdrawals in summer (especially at 140000 m<sup>3</sup> of storage capacity). In spring, evaporation is higher than withdrawals for most years, and is therefore an important loss term. In withdrawals are more than 3 times higher than evaporation, and also more variable between the simulations, which means that the withdrawals is certainly the main driver of the hydrological impacts of reservoirs in summer. There is a large annual variability of rainfall on reservoirs. However, the order of magnitude of seasonal rainfall and evaporation on reservoirs are the same, which means that these two terms compensate for each other over a year in average.

## S 4.2 Low flow at the outlet vs proportion of network in low flow

Figure S5 shows that the relationship between the annual number of low-flow days at the outlet and the annual proportion of network in low flow is coarse, even in the reference situation. Generally, the number of days with low-flow at the outlet increases with the proportion of network in low-flow, but the dispersion is high. Therefore, the number of low-flow days at the outlet is not a good proxy for the proportion of network in low flow and the proportion of network in low flow is preferred to describe the hydrological state of the stream. There is no relation either in the other seasons.

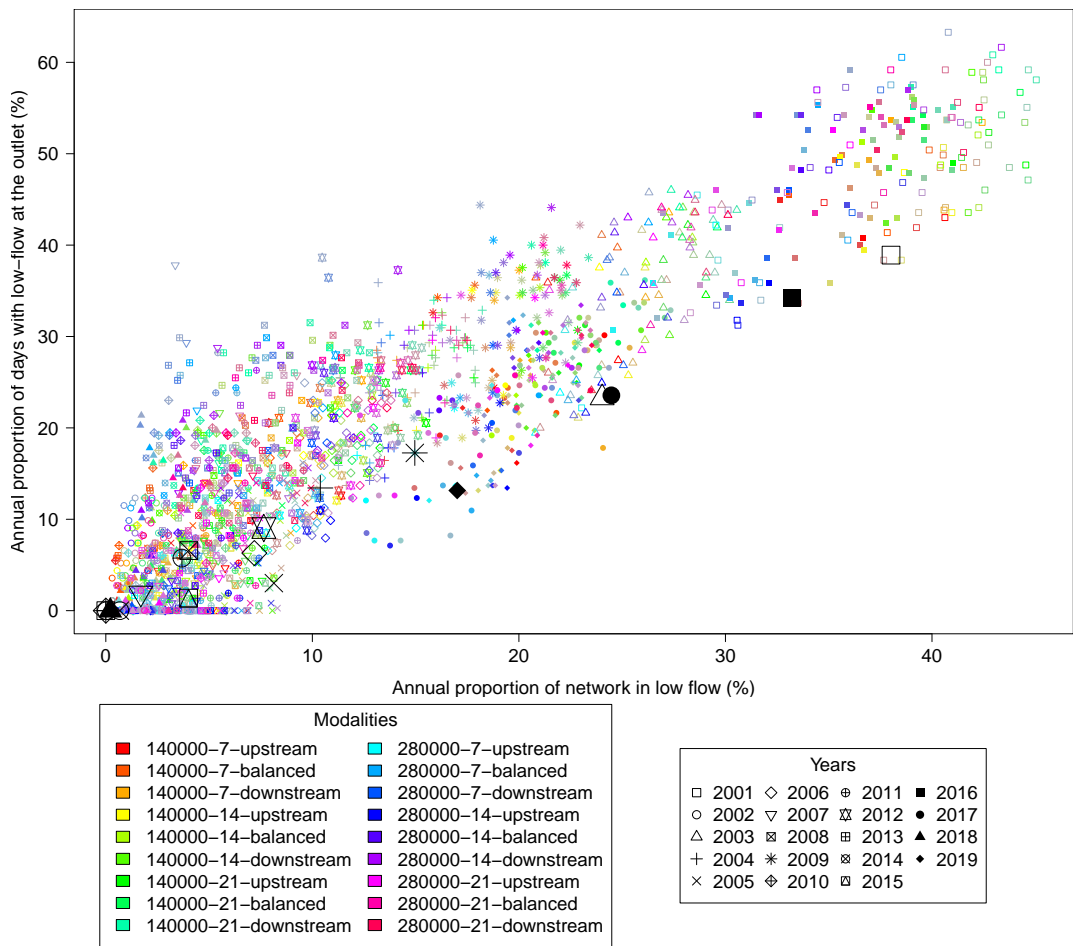


Figure S5: Comparison of the annual proportion of network in low flow and the number of low-flow days at the outlet (expressed in terms of % of total year days). The bigger black symbols are values in the reference situation.

## S 5 Minimum required flow vs low-flow threshold

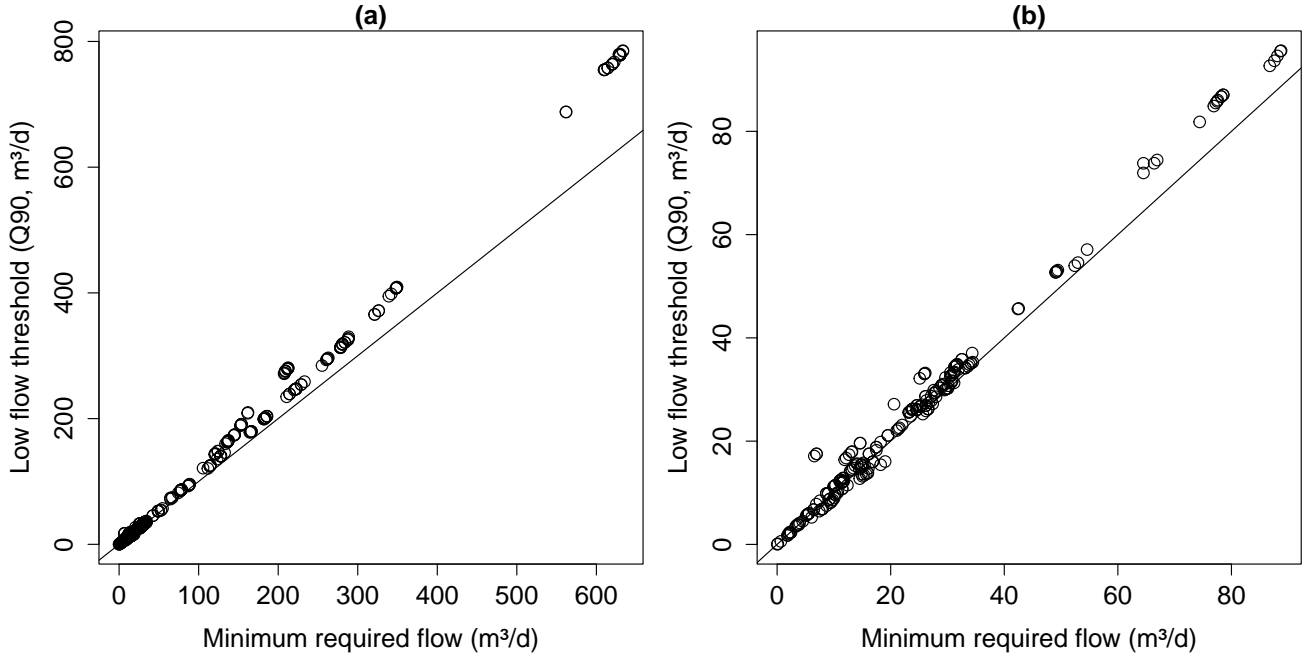


Figure S6: Comparison of the minimum required flow and the low flow threshold for each RS of the hydrological network: all RS (a), and zoom for RS with a minimum flow inferior to  $100 \text{ m}^3/\text{d}$  (b). The lines indicate the  $x=y$  curve.

There are two thresholds to characterize low flows in each point of the hydrological network :

- The minimum required flow: it represent the flow that a reservoir must legally let pass if upstream flows are not null. It is computed based on flow measurements at the closest downstream station, and values 10 % of the mean annual discharge at the gauging station adjusted with drained areas. When we place a reservoir in a random position of the network, we automatically calculate this minimum flow in  $\text{m}^3 \cdot \text{s}^{-1}$  with the following formula:  $0.1 \times \frac{\text{drained area (m}^2\text{)}}{19822640} \times 0.0733$ .
- The low-flow threshold: it represent the daily Q90 at the RS computed on the 20 years in the reference situation. It is used to calculate the proportion of network in low-flow.

In Figure S6, we can see that the two thresholds are different and not exactly related. This is normal since the method to calculate them is different. The minimum flow is usually lower than the low-flow threshold. This means that if a reservoir is located on such an RS, and that it is refilling, the flow that will be transmitted downstream (the minimum flow) will be inferior to the low-flow threshold, and downstream RS will be considered as in low flow with our indicator of low-flow proportion.

The values are different as both thresholds are defined for different purposes. The minimum required flow is a legal value that is computed with available data and must be applied. On the Gélon, the reference data comes from a downstream gauging station. The low-flow threshold is fixed to have a more rigorous approach to the characterization of the current hydrological state of the stream in our context of research.

Finally, in Figure S7, we see that the area drained by a RS can already be drained by the upstream RS, i.e. the contribution of runoff and baseflow directly in these RS is low. This means that, if a reservoir is placed upstream of the RS, the only discharge going through the RS comes from the reservoir. These RS are more likely to be impacted by the presence of a reservoir.

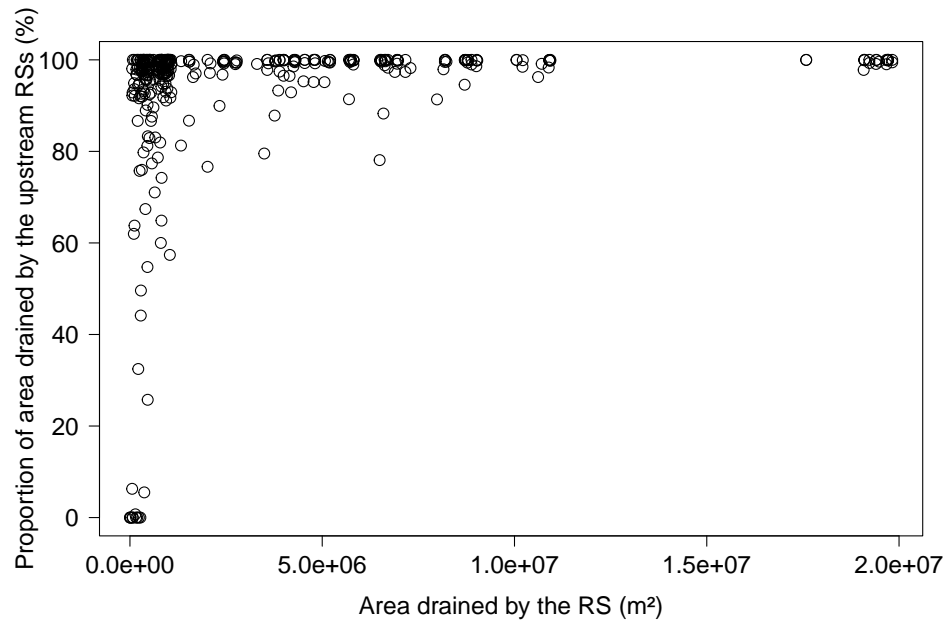


Figure S7: Proportion of area drained by a RS that is also drained by the upstream RSs.

## References

- J. Liebe, N. van de Giesen, and M. Andreini. Estimation of small reservoir storage capacities in a semi-arid environment: A case study in the Upper East Region of Ghana. *Physics and Chemistry of the Earth, Parts A/B/C*, 30(6):448–454, January 2005. ISSN 1474-7065. doi: 10.1016/j.pce.2005.06.011.
- Clément Murgue, Romain Lardy, Maroussia Vavasseur, Delphine D Burger-Leenhardt, and Olivier Therond. Fine spatio-temporal simulation of cropping and farming systems effects on irrigation withdrawal dynamics within a river basin. Santiago, United States, 2014. International Environmental Modeling and Software Society (iEMSs).
- Arthur N. Strahler. Quantitative analysis of watershed geomorphology. *Eos, Transactions American Geophysical Union*, 38(6):913–920, 1957. ISSN 2324-9250. doi: 10.1029/TR038i006p00913.